Surface and mechanical properties of plasma-modified chitosan/polyvinyl alcohol composite films

Shih-Hang Chang[1), *)] (ORCID ID: 0000-0002-2262-0396), **Yuan-Hsuan Chang**[1)]

DOI: https://doi.org/10.14314/polimery.2025.3.3

Abstract: The surface and mechanical properties of chitosan/polyvinyl alcohol (CS/PVA) composite films modified with O_2 and N_2 plasma were investigated. The FT-IR method confirmed the presence of characteristic bands originating from both CS and PVA, the intensity of which significantly increased after plasma modification. Plasma treatment also increased the hydrophilicity of CS/PVA films, with a slight decrease in their surface smoothness. In addition, plasma modification reduced the adhesion of bovine serum albumin. The highest fracture toughness and the lowest adhesion of bovine serum albumin were obtained for CS/PVA films (1/3 wt%/wt%). The conducted studies confirmed the possibility of biomedical applications of chitosan/polyvinyl alcohol composite films.

Keywords: chitozan, polyvinyl alcohol, composites, plasma modification, biomedical applications.

Właściwości powierzchniowe i mechaniczne folii kompozytowych chitozan/alkohol poliwinylowy modyfikowanych plazmą

Streszczenie: Zbadano właściwości powierzchniowe i mechaniczne folii kompozytowych chitozan/alkohol poliwinylowy (CS/PVA) modyfikowanych plazmą O_2 i N_2. Metodą FT-IR potwierdzono obecność charakterystycznych pasm pochodzących zarówno od CS, jak i PVA, których intensywność znacząco zwiększyła się po modyfikacji plazmą. Działanie plazmy zwiększyło również hydrofilowość folii CS/PVA, przy niewielkim zmniejszeniu gładkości ich powierzchni. Ponadto modyfikacja plazmą zmniejszyła adhezję albuminy surowicy bydlęcej. Największą wytrzymałość na pękanie i najmniejszą adhezję albuminy surowicy bydlęcej uzyskano w przypadku folii CS/PVA (1/3 % mas./% mas.). Przeprowadzone badania potwierdziły możliwość biomedycznych zastosowań folii kompozytowych chitozan/alkohol poliwinylowy.

Słowa kluczowe: chitozan, alkohol poliwinylowy, kompozyty, modyfikacja plazmą, zastosowania biomedyczne.

Metallic biomaterials, such as stainless steel, cobalt-chromium alloys, titanium alloys, molybdenum alloys, and shape memory alloys, are widely used as surgery prosthetics, dental implants, bone plates, screws, stents, and cardiovascular devices. Although these metallic biomaterials exhibit good biocompatibility, they may release metal ions when used in long-term implants [1]. For instance, stainless steel implants may release chromium and nickel ions, which can cause allergic reactions and tissue damage. Therefore, the surfaces of implant materials are usually protected by various coatings, such as those of polymers, bioactive glasses, and biocompatible ceramics, to prevent the corrosion of implants and the leaching of potentially toxic metal ions [2–6]. Polyvinyl alcohol (PVA) and chitosan (CS) are particularly attractive for biomedical coatings because they have excellent biocompatibility and are non-toxic and economical.

PVA has been widely used for biomedical engineering applications, including tissue mimicking, vascular cell culturing, and vascular implantation, because of its non-toxic, hydrophilic, biodegradable, and biocompatible properties. Besides, PVA is flexible and can form thin films, because of which PVA films are suitable for the surface modification of biomedical implants [7–10]. Nevertheless, the poor mechanical properties of PVA typically restrict its practical applications. Several studies have demonstrated that the incorporation of inorganic additive nanofillers into PVA films can enhance their mechanical properties [11–14]. However, the additive nanofillers can decrease the biocompatibility of PVA and limit its medical applications. Chitosan, a versatile bioactive polymer with abundant hydroxyl and amino groups, is also suitable for biomedical applications. It is non-toxic, biocompatible, biodegradable, and economical material, which also exhibits antibacterial and antifungal activity with good mechanical properties [15–18]. Nevertheless, the highly hydrophobic nature of chitosan may be disadvantageous for their anticoagulant properties and may restrict their

[1)] Department of Chemical and Materials Engineering, National I-Lan University, I-Lan 260, Taiwan.

[*)] Author for correspondence: shchang@niu.edu.tw

corresponding biochemical functions. Therefore, numerous studies have investigated the hydrophilic modifications of chitosan to optimize its benefits and biomedical applications [19–24].

Chitosan and PVA polymers exhibit good miscibility because of their unique intermolecular interactions [25]. The addition of PVA into the CS matrix can improve the hydrophilicity of the composite film because of the highly hydrophilic nature of PVA. Additionally, blending CS with PVA can enhance the mechanical properties of the composite film owing to the formation of hydrogen bonding and electrostatic interactions [26]. CS/PVA composite films have been applied to CO_2 separation, heavy metal filtration, dye adsorption, and functional food packaging. In addition, the CS/PVA composite is regarded as a potential biomaterial because of its excellent biocompatibility, high blood compatibility, and antibacterial properties. Several studies have reported that the CS/PVA composite is promising for tissue engineering applications because of its good biocompatibility, versatility, and ability to support cell growth and tissue regeneration [26–28]. Besides, the CS/PVA composite exhibits significant potential for modern wound dressing because of its antibacterial and adhesive hemostatic properties [29–31].

Nevertheless, the applications of CS/PVA composites for implant protective coatings requiring good blood anticoagulant properties have not been studied before. Therefore, this study aimed to investigate the surface properties and anti-protein adsorption characteristics of the CS/PVA composite films. Recently, Paneru *et al*. [32] have reported that the antibacterial properties and wettability of the CS/PVA composite film surface can be improved using non-thermal atmospheric pressure plasma. Therefore, a preliminary assessment of the potential biomedical applications of the plasma-modified CS/PVA composite films was conducted in this study.

EXPERIMENTAL PART

Materials

CS powder used in this study was prepared from crab shells and was purchased from C&B Co. Ltd., (Taichung, Taiwan). The CS powder had a molecular weight of 10–50 kDa, with a deacetylation degree of 90%. PVA powder was purchased from First Cosmetics Works (Taoyuan, Taiwan).

Composite films preparation

Individually, 0.5, 1, and 1.5 g of the PVA powder was mixed with 100 mL of deionized water in a beaker to obtain PVA solutions of various concentrations. Each solution was stirred at 500 rpm and 90°C for 60 min. After cooling to room temperature, 1.5, 1, and 0.5 g of the CS powder was added to the PVA solutions containing 0.5, 1, and 1.5 g of PVA, respectively, to obtain CS/PVA gels with various weight ratios [CS/PVA (3/1), (1/1), and (1/3) g/g]. Each CS/PVA gel was stirred at 500 rpm and 90°C for 180 min. Then, the CS/PVA gels were allowed to stand for 12 h at room temperature, following which they were poured into a stainless-steel tray and dried in an oven at 37°C to afford dense, ~50-μm thick CS/PVA composite films. Neat CS and PVA films were also prepared for comparison.

Plasma modification

The surfaces of selected CS/PVA composite films were further modified by O_2 and N_2 plasma. The plasma system used in this study was custom manufactured by Chintech Technology Co. (Dongguan China), using a radiofrequency (RF) generator equipped with a Pyrex bell-jar reactor. The frequency of the RF generator was set to 13.56 MHz. The cathode was connected to the high-potential end of the RF generator, and the anode was grounded. The CS/PVA composite films were placed on the anode. The distance between the cathode and anode was set to 100 mm. After the system was evacuated to a base pressure of 10^{-3} Torr or lower, high-purity O_2 or N_2 was introduced into the chamber, following which the pressure was adjusted to a stable working pressure of 0.125 Torr with a flow rate of ten sccm. The plasma modification was performed at a constant power of 50 W for 10 min.

Methods

The functional groups of the CS/PVA composite films were detected by attenuated total reflectance Fourier-transform infrared spectroscopy (ATR FT-IR) (Spectrum 100, PerkinElmer, Waltham, MA, USA). Each specimen was assessed in the range of 4,000–400 cm^{-1} and 16 scans were obtained at a resolution of 4 cm^{-1}. The wettability of the CS/PVA composite film surfaces was measured by the sessile drop method using a contact angle instrument (FTA125, First Ten Angstroms, Newark, CA, USA). The average contact angle was calculated based on seven measurements at different locations on the film, omitting the maximum and minimum values. The surface morphology of the CS/PVA composite films was examined by scanning electron microscopy (SEM; 5136 MM, Tescan, Kotoutovice, Czech Republic). Before observing the morphology, each composite film was gold-coated using a vacuum sputter coater. The average roughness (Ra) of the CS/PVA composite film surfaces was determined by Atomic Force Microscopy (AFM; FM-Nanoview1000, FSM, China) in the tapping mode.

Tensile properties were determined using a universal testing machine (Instron 4469, Instron Corporation, Norwood, MA, USA) with a 1 kN load cell to evaluate the mechanical properties of the CS/PVA composite films at a constant strain rate of 10 mm/min. Young's modu-

lus was obtained from the fitting line of the linear portion of the stress–strain curve, and the toughness was determined from the area under the stress–strain curve. The anticoagulant properties of the CS/PVA composite films were assessed by determining the amount of protein adsorbed on the film surface using the bicinchoninic acid (BCA) protein assay. The protein used in the BCA assay was bovine serum albumin (BSA). Both BSA and BCA were purchased from Bio Basic Inc. (Markham, Canada). Phosphate buffered saline (PBS), and sodium dodecyl sulfate (SDS) used in the protein adsorption analyses were purchased from UniRegion, Taiwan and Sigma-Aldrich, USA, respectively. In the protein adsorption analysis, the optical density (OD) was measured at 562 nm on a spectrophotometer (GENESYS 20, Thermo Scientific, Waltham, MA, USA) using a PBS solution as the blank.

RESULTS AND DISCUSSION

ATR FT-IR analysis

ATR-FT-IR spectra of the neat CS, neat PVA, and CS/PVA composite films with various CS/PVA weight ratios are shown in Fig. 1. As shown in Fig. 1, the neat CS film exhibited a broad characteristic peak at 3100–3500 cm^{-1}, attributable to the –OH and $–NH_2$ stretching vibrations. The characteristic absorption band at approximately 2900 cm^{-1} was attributed to the –CH group. The characteristic absorption bands at approximately 1655, 1555, and 1400 cm^{-1} were attributed to the –C=O carbonyl stretching of amide I, –NH bending of amide II, and–CN stretching of amide III, respectively. The absorption band at 1000–1100 cm^{-1} was attributed to the –CO functional group.

The neat PVA film exhibited an absorption band between 3100 and 3500 cm^{-1}, which was attributed to the intermolecular hydrogen bonding and −OH single vibration of PVA. The characteristic absorption bands at approximately 2900 and 1100 cm^{-1} were attributed to the C–H stretching vibration and C–O bond of PVA, respectively. The characteristic absorption bands at 1400 and 1300 cm^{-1} were attributed to the twisting of the $–CH_3$ group of PVA. Figure 1 also shows that all the CS/PVA composite films with varying CS/PVA weight ratios exhibited the characteristic absorption peaks of both CS and PVA.

Water contact angle measurements

The water contact angles of the neat CS, neat PVA, and CS/PVA composite films with various CS/PVA weight ratios are shown in Fig. 2. Figure 2 indicates that the neat CS film exhibited a high-water contact angle of approximately 93.4±0.6° owing to its hydrophobic nature. In contrast, the neat PVA film exhibited a low water contact angle of approximately 23.8±1.3° because of the abundant hydrophilic functional groups on its surface. Figure 2 also shows that the water contact angles of the CS/PVA composite films gradually decreased with the amount of PVA in these films—the CS/PVA (1/3) composite film exhibited the best hydrophilic property among the tested composite films.

SEM and AFM analysis

The SEM images of the neat CS film, CS/PVA (3/1) composite film, CS/PVA (1/1) composite film, CS/PVA (1/3) composite film, and neat PVA film are presented in Fig. 3a–e, respectively. Fig. 3a–e revealed that the neat CS and PVA films had a smooth surface morphology. Fig. 3b–d shows that the various CS/PVA composite films also had a homogeneous and smooth surface, indicating that PVA and CS were homogeneously mixed in the CS/PVA composite films. The AFM 3D images of the neat CS film, CS/PVA composite films, and neat PVA film are shown in Fig. 4. It is evident that the neat CS, neat PVA, and CS/PVA composite films exhibited a flat surface morphology, with only some random protuberances on the surface. According to Fig. 4, the Ra values of the neat CS film, neat PVA film,

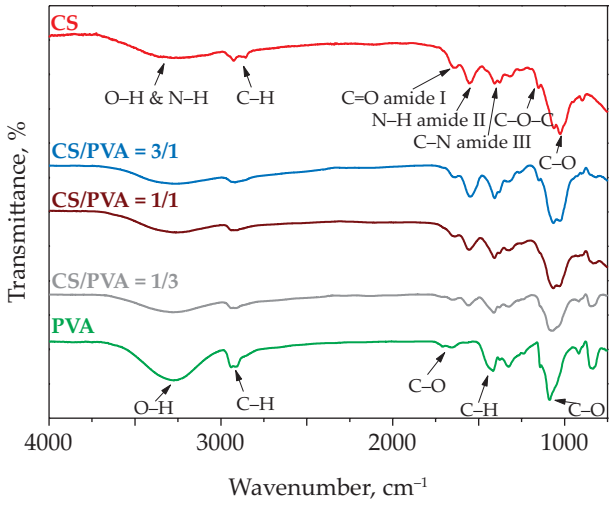

Fig. 1. ATR-FT-IR spectra of tested composite films

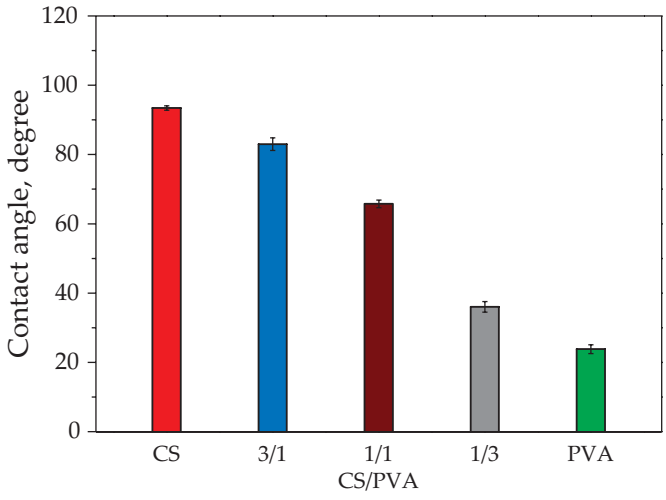

Fig. 2. Water contact angle of tested composite films

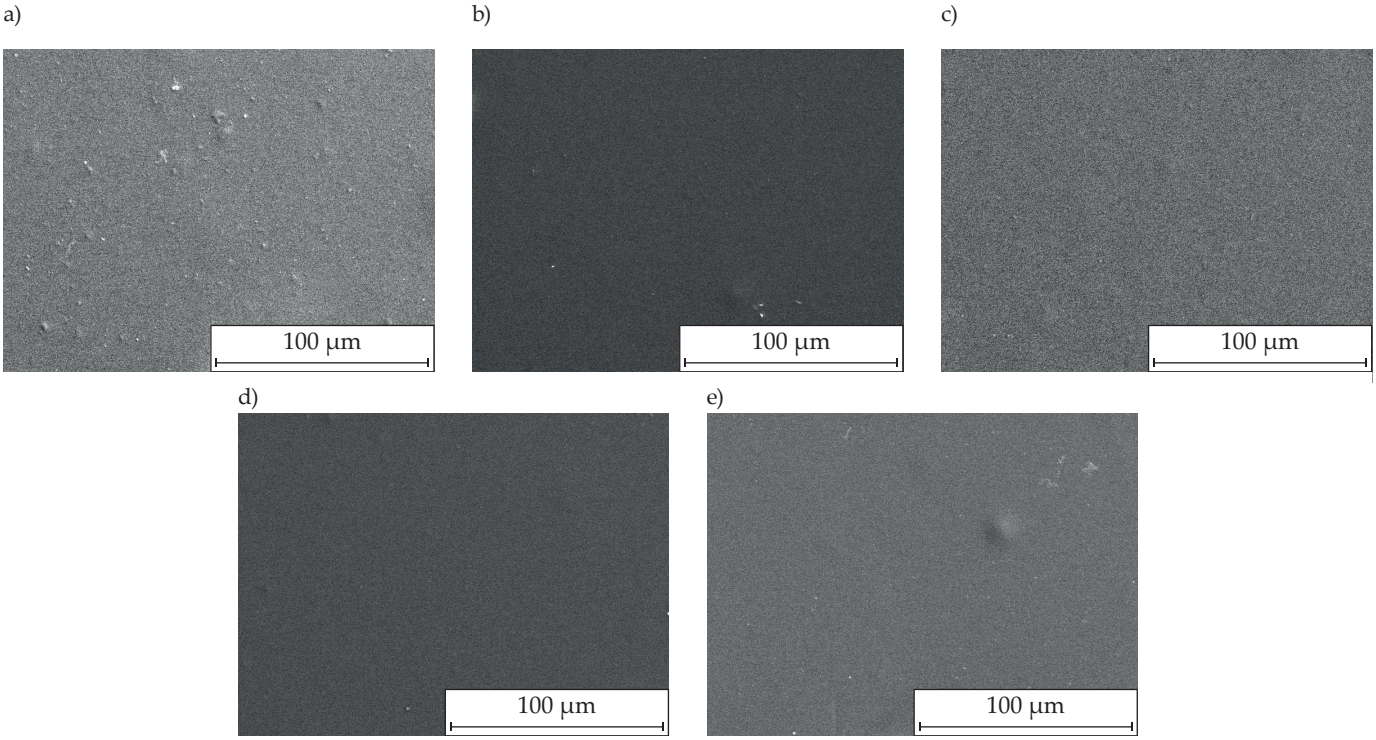

Fig. 3. SEM images: a) neat CS film, b) CS/PVA (3/1) composite film, c) CS/PVA (1/1) composite film, d) CS/PVA (1/3) composite film, e) neat PVA film; 1000× magnification

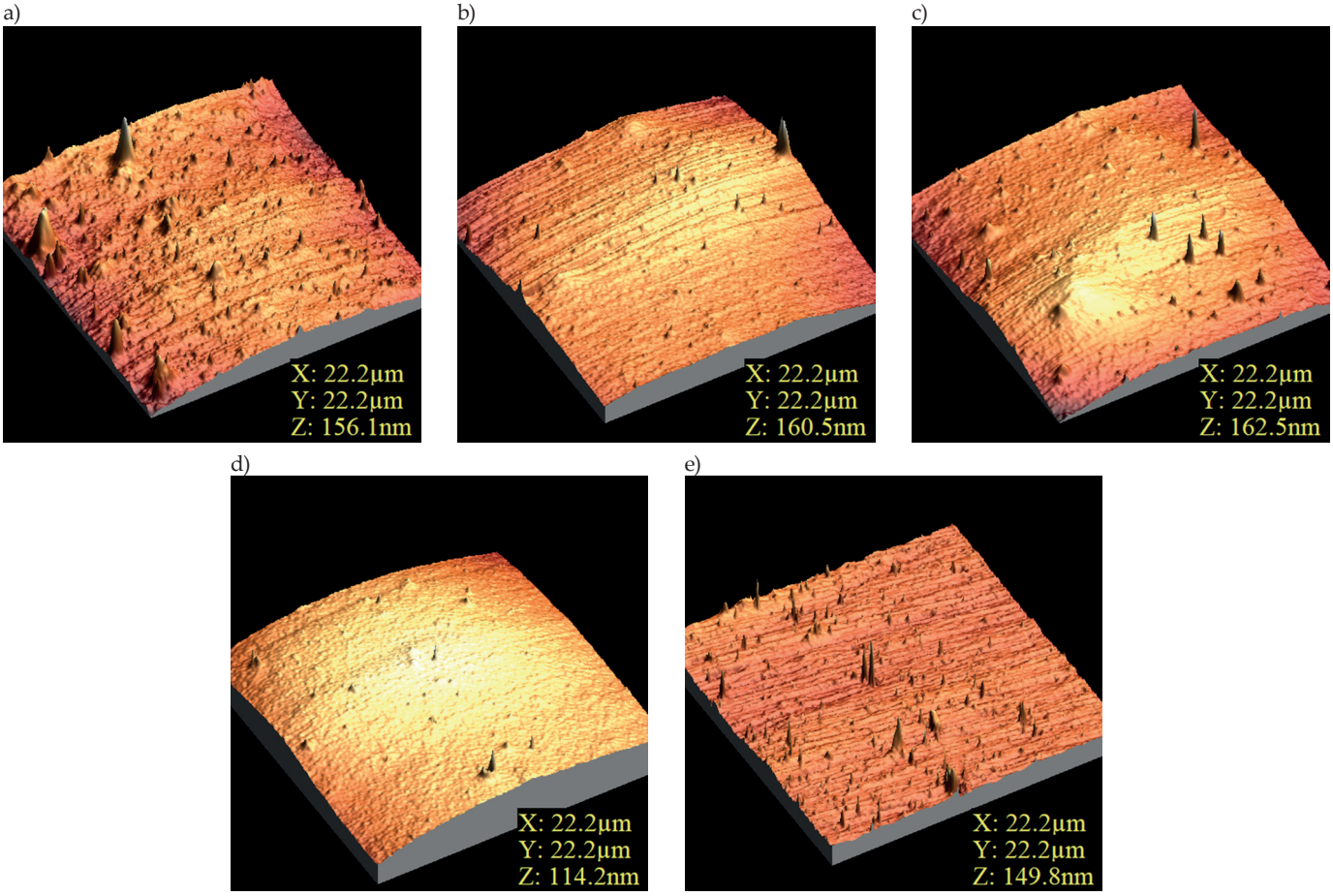

Fig. 4. AFM images: a) neat CS film, b) CS/PVA (3/1) composite film, c) CS/PVA (1/1) composite film, d) CS/PVA (1/3) composite film, e) neat PVA film

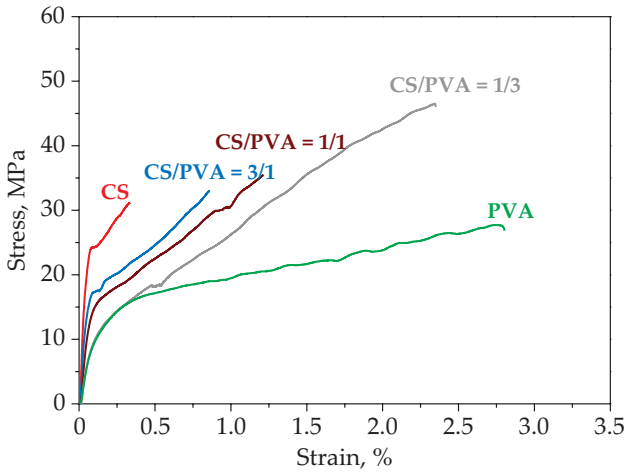

Fig. 5. Stress–strain curves of tested composite films

CS/PVA (3/1) composite film, CS/PVA (1/1) composite film, and CS/PVA (1/3) composite film were 11.9±2.9, 8.2±1.6, 13.2±1.2, 12.0±2.9, and 11.9±2.3 nm, respectively.

Mechanical properties

The tensile stress–strain curves of neat CS film, CS/PVA composite films, and neat PVA film are shown in Fig. 5a–e. For a clear comparison, Figure 5f shows the overlapped tensile stress–strain curves selected from each specimen in Fig. 5a–e for clear comparison. Fig. 5a–e shows that the stress–strain curves of each specimen were remarkably similar, indicating that all the CS/PVA composite films were highly homogenous. In contrast, as shown in Fig. 5f, the tensile test results were notably different for these specimens.

The fracture strain, Young's modulus (E), and fracture toughness, respectively, of each specimen shown in Fig. 5 are plotted in Fig. 6. Young's modulus is determined by the slope of the best-fit line in the stress–strain curve. The fracture toughness is determined by calculating the total area under the stress–strain curve up to the point of failure. Figure 6a shows that the neat PVA film possessed the largest fracture strain of approximately 2.8±0.2 MPa, while the neat CS film exhibited a low fracture strain of approximately 0.4±0.1 MPa because of its brittle nature. For the CS/PVA composite films, the fracture strain values of the specimens increased gradually with increasing PVA content in the composite films. Figure 6b shows that the neat CS film exhibited a higher Young's modulus of approximately 693±130 MPa, whereas the neat PVA film exhibited a low Young's modulus of approximately 112±26 MPa. The Young's modulus values of the CS/PVA composite films decreased gradually with increasing PVA content in the composite films.

Although the neat CS film exhibited the largest Young's modulus among the specimens assessed, its fracture toughness value was only approximately 11.4±2.8 MJ/m^3 (Fig. 6c) because of its extremely low fracture strain. Compared to the neat CS film, the neat PVA film exhibited a much larger fracture toughness value of approximately 57.2±2.9 MJ/m^3 because of its larger fracture strain. According to Fig. 6(c), the fracture toughness values of the CS/PVA (3/1), CS/PVA (1/1), and CS/PVA (1/3) composite films were 20.3±2.9, 30.9±1.6, and 68.7±6.4 MJ/m^3, respectively. The CS/PVA (1/3) composite film exhibited the highest fracture toughness amongst all the neat and composite materials assessed, indicating that this CS/PVA composite film combined the advantages of the ductility of PVA and the deformation resistance of CS.

Protein adsorption properties

The protein adsorption properties of the neat CS, neat PVA, and CS/PVA composite films were determined using the BCA protein assay. Each film specimen was rinsed three times with PBS, immersed in 5 mL of a BSA solution at 37°C for 24 h, and then rinsed again with PBS. Next, the rinsed films were immersed in 2 mL of an SDS solution for 24 h. A 0.1 mL aliquot of each sample solution was mixed with 1 mL of the BCA solution in a cuvette to determine its OD using a spectrophotometer. The concentration of BSA adhered to the films was calculated from the OD values using a standard BSA concentration curve.

The concentrations of the BSA adhered to the different CS/PVA composite films are shown in Fig. 7. As shown in Fig. 7, the concentrations of BSA adhered to the surface of the neat CS and PVA films were 53.9±3.2 and 36.0±2.3 μg/mL, respectively. The concentrations of BSA adhered to the surfaces of the CS/PVA (3/1), CS/PVA (1/1), and CS/PVA (1/3) composite films were 45.3±2.6, 39.3±2.6, and 38.7±3.3 μg/mL, respectively.

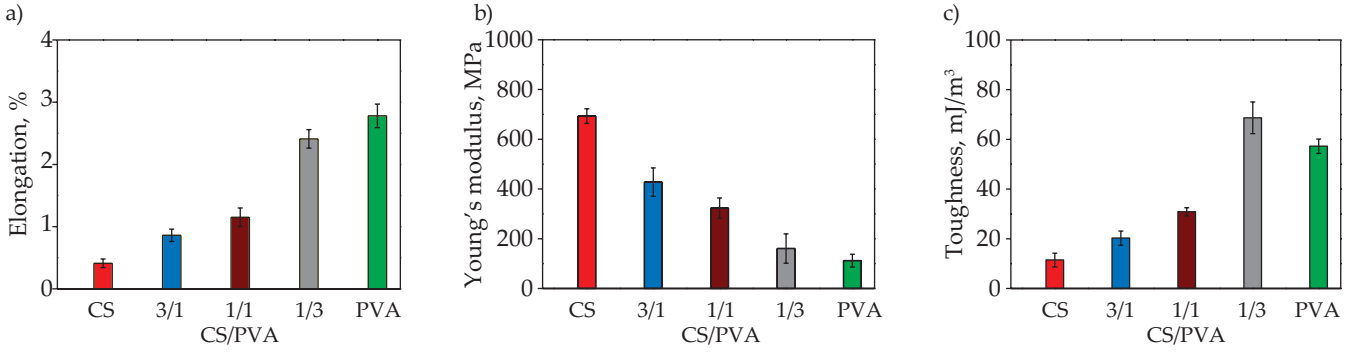

Fig. 6. Selected mechanical properties of examined films: a) elongation at break, b) Young's modulus, c) toughness

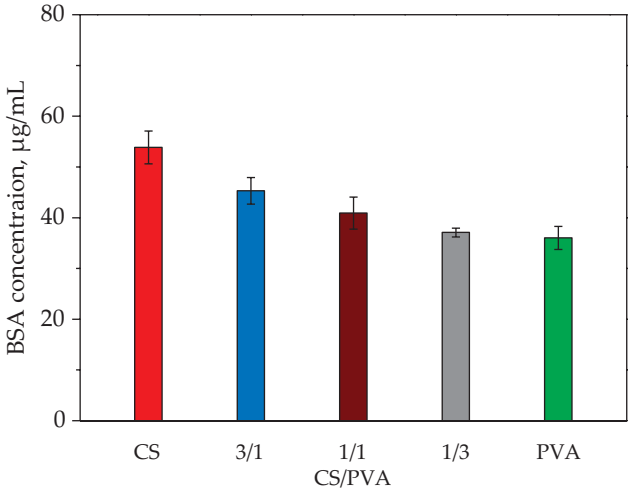

Fig. 7. BSA adsorption concentrations on examined films

As shown in Fig. 7, the neat CS film exhibited a higher concentration of absorbed BSA because the carboxylic acid group of BSA easily formed hydrogen bonds with the abundant carbonyl and amid functional groups of the CS film. On the other hand, the neat PVA film exhibited a lower concentration of adsorbed BSA because its highly hydrophilic surface inhibited BSA adsorption [33]. The amount of BSA adhered to the surface of the CS/PVA composite films was intermediate between the amounts adhering to the neat CS and PVA films, and it gradually decreased with increasing PVA content in the composite films.

Plasma modification

To improve the surface properties of the CS/PVA composite films, the CS/PVA (1/3) composite films were further subjected to O_2 and N_2 plasma modification. The CS/PVA (1/3) composite film was selected because the amount of adhered BSA was the least and the fracture toughness was the highest for this film among the CS/PVA composite films studied. The ATR-FTIR spectra of the unmodified CS/PVA (1/3) composite film and the O_2 and N_2 plasma-modified CS/PVA (1/3) composite films

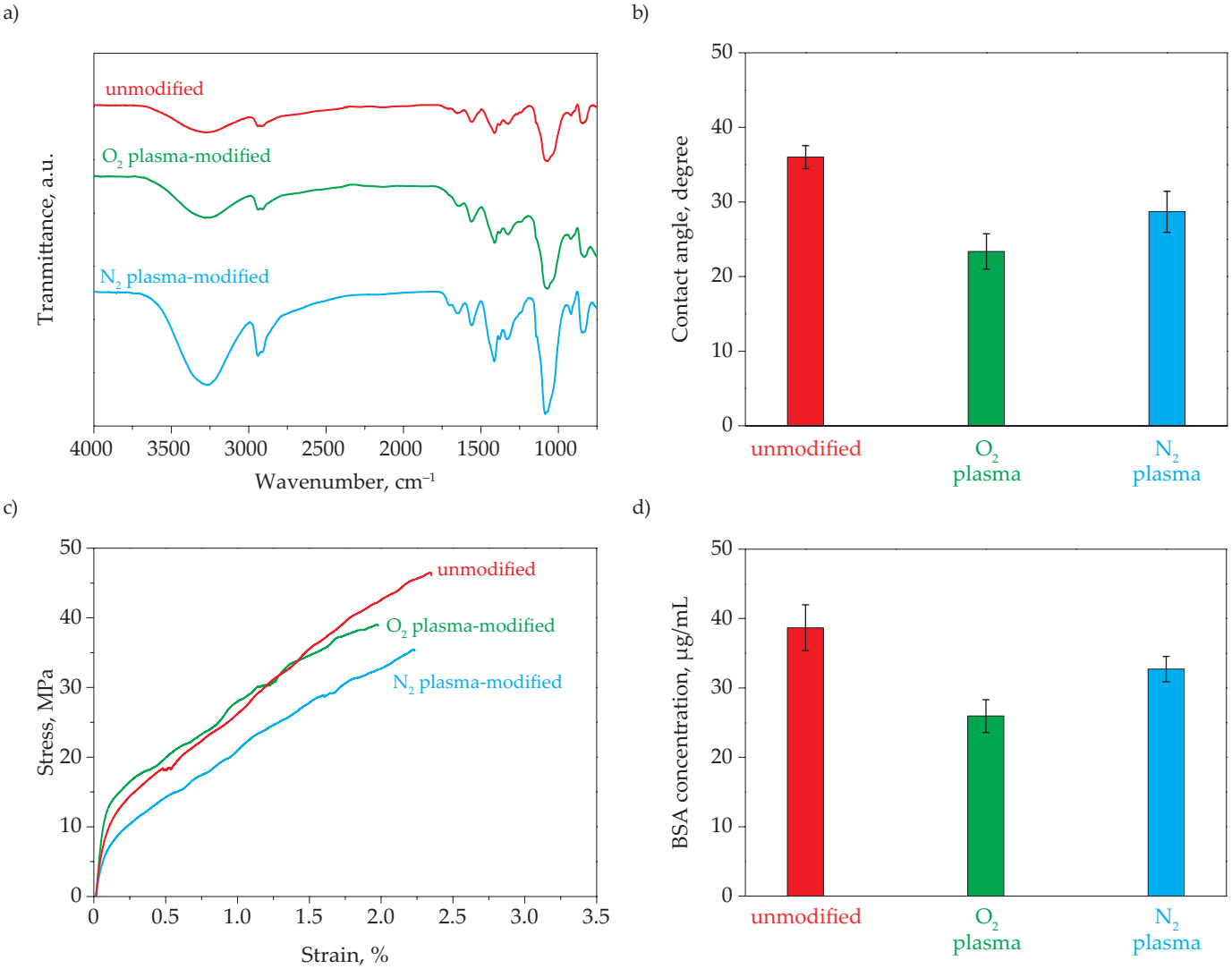

Fig. 8. Selected properties of modified and unmodified composite films: a) ATR FT-IR spectra, b) water contact angle, c) tensile stress-strain curves, d) BSA adsorption concentrations

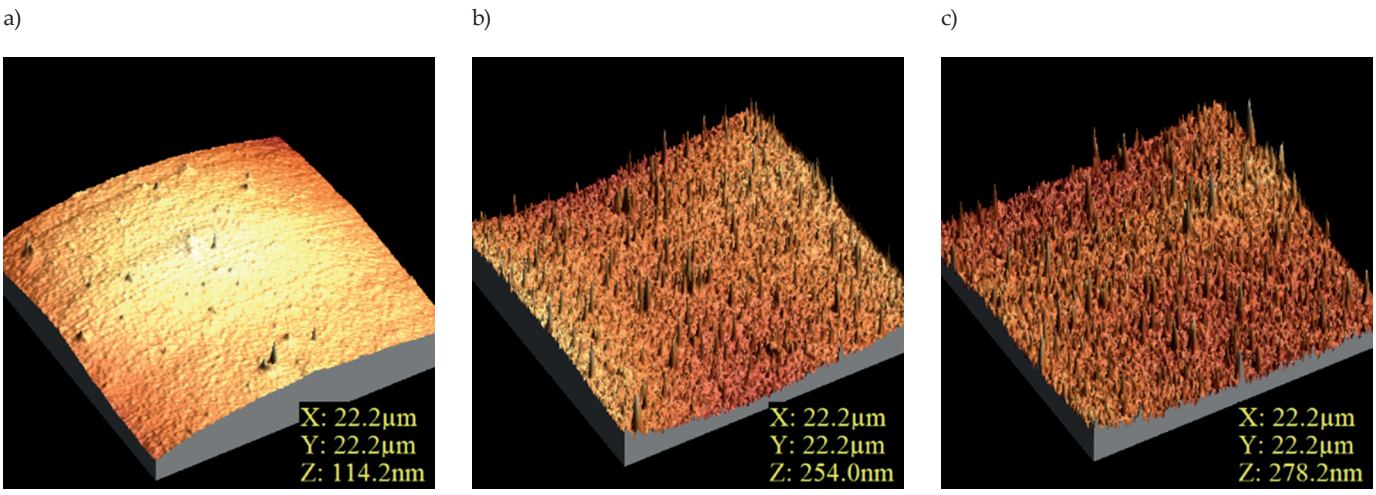

Fig. 9. AFM images of CS/PVA (1/3) composite films: a) unmodified, b) O_2 plasma-modified, c) N_2 plasma-modified

are shown in Fig. 8a. According to Fig. 8a, the characteristic peaks of the CS/PVA (1/3) composite film, particularly the –OH and $–NH_2$ stretching vibration peaks at approximately 3100–3500 cm^{-1} and the C–O stretching vibration peak at approximately 1100 cm^{-1}, became more intense after O_2 and N_2 plasma modification This is because of the functionalization with O- and N-containing groups during the plasma modification.

The water contact angles of the unmodified CS/PVA (1/3) composite film and the corresponding O_2 and N_2 plasma-modified composite films Fig. 8b. As shown in Fig. 8b, O_2 and N_2 plasma modifications reduced the water contact angle of this composite film (36.0±1.5°) to approximately 28.7±2.8° and 23.4±2.4°, respectively. This indicated that the surface of the CS/PVA (1/3) composite film became more hydrophilic after O_2 and N_2 plasma modifications, which can be attributed to the increased number of the hydrophilic functional groups during the plasma modifications (Fig. 8a). The tensile stress–strain curves of the unmodified CS/PVA (1/3) composite film and the corresponding O_2 and N_2 plasma-modified composite films are shown in Fig. 8c. As shown in Fig. 8c, the stress–strain curves of the unmodified and plasma-modified CS/PVA (1/3) composite films were not significantly different, indicating that the mechanical properties of the CS/PVA composite films did not deteriorate after the plasma modifications.

The BSA adhesion concentrations of the unmodified CS/PVA (1/3) composite film and the corresponding O_2 and N_2 plasma-modified composite films are shown in Fig. 8d. As shown in Fig. 8d, the concentrations of BSA adhered to the surface of the CS/PVA (1/3) composite film (38.7±3.3 µg/mL) reduced to approximately 32.7±1.8 and 25.9±2.4 µg/mL after O_2 and N_2 plasma modifications, respectively. According to the significance analysis, the P-values calculated from the BSA adhesion concentration results were approximately $1.76 \cdot 10^{-3}$ and $9.05 \cdot 10^{-3}$ after O_2 and N_2 plasma modifications, respectively, indicating that the decrease in the BSA adhesion concentration upon O_2 or N_2 plasma modification was highly significant ($P<<0.05$). Accordingly, we concluded that both O_2 and N_2 plasma modifications effectively improved the protein adsorption property of the CS/PVA (1/3) composite film (highly significant).

Although the N_2 and O_2 plasma-modified CS/PVA (1/3) composite films possessed abundant hydroxyl functional groups on the surface and exhibited high hydrophilicity, the water contact angle and the amount of BSA adsorbed on the N_2 plasma-modified composite film were both slightly lower than those for the O_2 plasma-modified composite film. This feature may be due to the etching effect of the high-energy O_2 and N_2 plasmas. Figure 9a–c shows the AFM images of the unmodified CS/PVA (1/3) composite film and the corresponding O_2 and N_2 plasma-modified composite films, respectively. The unmodified CS/PVA (1/3) composite film exhibited a smooth morphology, whereas the surface of the corresponding O_2 and N_2 plasma-modified composite films had abundant notches, spots, and cone-like protuberances. The Ra values of the unmodified CS/PVA (1/3) composite film and the corresponding O_2 and N_2 plasma-modified composite films were 11.9±2.3, 15.7±2.6, and 23.5±3.6 nm, respectively. This indicated that the surface of the CS/PVA (1/3) composite film became rougher after O_2 and N_2 plasma modifications. Besides, the surface of the N_2 plasma-modified CS/PVA (1/3) composite film was slightly rougher than that of the O_2 plasma-modified CS/PVA (1/3) composite film, suggesting that the etching effect of the former modification on the surface of the CS/PVA composite film was more significant than that of the latter modification. This may be responsible for the slightly higher BSA adsorption on the O_2 plasma-modified composite film (Fig. 8d). Nevertheless, the N_2 and O_2 plasma-modified CS/PVA composite films showed a superior anti-protein adsorption property compared to the unmodified CS/PVA composite film, indicating that the N_2 and O_2 plasma-modified CS/PVA composite films are suitable for the surface modification of metallic implant materials. According to our studies, plasma-modified CS/PVA composite films are suitable for biomedical applications because of their

superior mechanical properties, hydrophilicity, and anti-protein adsorption properties. However, further details on the biocompatibility of the CS/PVA composite films and the surface adhesion property of the CS/PVA composite films with implant materials still need to be clarified in the future.

CONCLUSIONS

The surface and mechanical properties of the CS/PVA composite films were investigated. The CS/PVA composite films showed characteristic absorption peaks of both CS and PVA in the FT-IR spectra. The characteristic peaks of hydrophilic functional groups on the surface of the CS/PVA (1/3) composite film became more intense after O_2 and N_2 plasma modification. The water contact angle and BSA protein adhesion ability of the CS/PVA composite films gradually decreased with the increase of PVA content in the CS/PVA composite films. The CS/PVA (1/3) composite film had the most hydrophilic surface and the lowest BSA adhesion ability among the evaluated CS/PVA composite films. Moreover, the Young's modulus of the CS/PVA composite films gradually decreased with the increase of PVA content in the composite. On the other hand, the fracture strain of the CS/PVA composite films increased simultaneously. The CS/PVA (1/3) composite film showed the highest fracture toughness among the evaluated CS/PVA composite films. The water contact angle and BSA adhesion concentration on the surface of the CS/PVA composite film were effectively reduced after modification with O_2 or N_2 plasma, without affecting the mechanical properties of the composite film. The water contact angle and BSA adsorption amount on the N_2 plasma-modified composite film were slightly lower than those on the O_2 plasma-modified composite film because the surface of the former film was slightly rougher than that of the latter film.

ACKNOWLEDGEMENTS

The authors gratefully acknowledge the financial support for this research provided by the National Science and Technology Council (NSTC), Taiwan, under Grant NSTC 112-2221-E-197-014-MY2.

Authors contribution

S.H.C. – research concept, methodology, investigation, validation, visualization, writing, supervision, funding acquisition; Y.H.C. – methodology, investigation, data curation, visualization.

Funding

The research was funded by the National Science and Technology Council under Grant NSTC 112-2221-E-197-014-MY2.

Conflict of interest

The authors declare that they have no known competing financial interests or personal relationships that could have appeared to influence the work reported in this paper.

REFERENCES

[1] Takamura K., Hayashi K., Ishinishi N. *et al.*: *Journal of Biomedical Materials Research* **1994**, *28(5)*, 583. https://doi.org/10.1002/jbm.820280508

[2] Hu X., Wang T., Li F. *et al.*: *RSC Advances* **2023**, *13*, 20495. https://doi.org/10.1039/D3RA02248J

[3] Oliver J.N., Su Y., Lu X. *et al.*: *Bioactive Materials* **2019**, *4*, 261. https://doi.org/10.1016/j.bioactmat.2019.09.002

[4] Santos-Coquillat A., Martínez-Campos E., Mora Sánchez H. *et al.*: *Surface and Coatings Technology* **2021**, *422*, 127508. https://doi.org/10.1016/j.surfcoat.2021.127508

[5] Chang S.H., Huang, J.J.: *Surface and Coatings Technology* **2012**, *206(23)*, 4959. https://doi.org/10.1016/j.surfcoat.2012.05.121

[6] Chang S.H., Chen J.Z., Hsiao S.H. *et al.*: *Applied Surface Science* **2014**, *289*, 455. https://doi.org/10.1016/j.apsusc.2013.11.004

[7] Bose S., Akbarzadeh Khorshidi M., Lally C.: *Journal of the Mechanical Behavior of Biomedical Materials* **2025**, *161*, 106787. https://doi.org/10.1016/j.jmbbm.2024.106787

[8] Zhu M., Zhang S., Li X. *et al.*: *Materials Today Communications* **2025**, *43*, 111760. https://doi.org/10.1016/j.mtcomm.2025.111760

[9] Teodorescu M., Bercea M., Morariu S.: *Biotechnology Advances* **2018**, *37(1)*, 109. https://doi.org/10.1016/j.biotechadv.2018.11.008

[10] Chang S.H., Tung K.W., Liao B.S. *et al.*: *Surface and Coatings Technology* **2019**, *362*, 208. https://doi.org/10.1016/j.surfcoat.2019.02.003

[11] Luo J., Ghaffar S., Chen W. *et al.*: *Polymer* **2023**, *284*, 126307. https://doi.org/10.1016/j.polymer.2023.126307

[12] Yi X., Yu W., Yan J. *et al.*: *Materials Today Communications* **2025**, *42*, 111287. https://doi.org/10.1016/j.mtcomm.2024.111287

[13] Jain N., Singh V.K., Chauhan S.: *Journal of the Mechanical Behavior of Biomedical Materials* **2017**, *26(5-6)*, 213. https://doi.org/10.1515/jmbm-2017-0027

[14] Meng L., Li J., Fan X. *et al.*: *Composites Science and Technology* **2023**, *232*, 109885. https://doi.org/10.1016/j.compscitech.2022.109885
[15] de Sousa Victor R., da Cunha Santos A.M., de Sousa B.V. *et al.*: *Materials* **2020**, *13(21)*, 4995. https://doi.org/10.3390/ma13214995
[16] Kou S., Peters L., Mucalo M.: *Carbohydrate Polymers* **2022**, *282*, 119132. https://doi.org/10.1016/j.carbpol.2022.119132
[17] Harugade A., Sherje A.P., Pethe A.: *Reactive and Functional Polymers* **2023**, *191*, 105634. https://doi.org/10.1016/j.reactfunctpolym.2023.105634
[18] Wang L., Xu Z., Zhang H. *et al.*: *European Polymer Journal* **2023**, *191*, 112059. https://doi.org/10.1016/j.eurpolymj.2023.112059
[19] Sajeev D., Rajesh A., Nethish Kumaar R. *et al.*: *Carbohydrate Research* **2025**, *548*, 109351. https://doi.org/10.1016/j.carres.2024.109351
[20] Chang S.H., Chian, C.H.: *Applied Surface Science* **2013**, *282*, 735. https://doi.org/10.1016/j.apsusc.2013.06.044
[21] Chang S.H., Liou J.S., Huang B.Y. *et al.*: *Surface and Coatings Technology* **2017**, *320*, 635. https://doi.org/10.1016/j.surfcoat.2016.10.031
[22] Chang S.H., Hsieh M.H.: *Polymers and Polymer Composites* **2021**, *29(9)*, 1442. https://doi.org/10.1177/0967391120968434
[23] Cohen E., Poverenov E.: *Chemistry – A European Journal* **2022**, *28(67)*, e202202156. https://doi.org/10.1002/chem.202202156
[24] Chang S.H., Kuan Y.T.: *Polymers and Polymer Composites* **2023**, *31*. https://doi.org/10.1177/09673911231187265
[25] Zhang W., Khan A., Ezati P. *et al.*: *Food Chemistry* **2024**, *443*, 138506. https://doi.org/10.1016/j.foodchem.2024.138506
[26] Nathan K.G., Genasan K., Kamarul T.: *Marine Drugs* **2023**, *21(5)*, 304. https://doi.org/10.3390/md21050304
[27] Benítez-Martínez J.A., Garnica-Palafox I.M., Rodríguez-Hernández A. *et al.*: *Applied Physics A* **2023**, *129*, 558. https://doi.org/10.1007/s00339-023-06821-9
[28] Grande-Tovar C.D., Castro J.I., Tenorio D.L. *et al.*: *Polymers* **2023**, *15(23)*, 4595. https://doi.org/10.3390/polym15234595
[29] Zhang Y., Jiang M., Zhang Y. *et al.*: *Materials Science and Engineering: C* **2019**, *104*, 110002. https://doi.org/10.1016/j.msec.2019.110002
[30] Zhang N., Zhang X., Zhu Y. *et al.*: *Polymers* **2023**, *15(22)*, 4362. https://doi.org/10.3390/polym15224362
[31] Alotaibi B.S., Khan A.K., Kharaba Z. *et al.*: *ACS Omega* **2024**, *9(11)*, 12825. https://doi.org/10.1021/acsomega.3c08856
[32] Paneru R., Ki S.H., Lamichhane P. *et al.*: *Applied Surface Science* **2020**, *532*, 147339. https://doi.org/10.1016/j.apsusc.2020.147339
[33] Tangpasuthadol V., Pongchaisirikul N., Hoven V.P.: *Carbohydrate Research* **2003**, *338(9)*, 937. https://doi.org/10.1016/S0008-6215(03)00038-7

Received 30 X 2024.
Accepted 6 I 2025.

Rapid Communications

Przypominamy Autorom, że publikujemy artykuły typu **Rapid Communications – prace oryginalne wyłącznie w języku angielskim** (o objętości 4–5 stron maszynopisu z podwójną interlinią, zawierające 2–3 rysunki lub 1–2 tabele), którym umożliwiamy szybką ścieżkę druku (do 3 miesięcy od chwili ich otrzymania przez Redakcję). Artykuł należy przygotować wg wymagań redakcyjnych zamieszczonych we wskazówkach dla P.T. Autorów.

* * *

We remind Authors that we publish articles of the **Rapid Communications** type – **the original papers, in English only** (with a volume of 4-5 pages of double-spaced typescript, containing 2–3 figures or 1–2 tables), which allow a fast print path (up to 3 months from when they are received by the Editorial Board). The article should be prepared according to the editorial requirements included in the Guide for Authors.